
Deciphering urban traffic impacts on air quality by deep learning and emission inventory

Wenjie Du^{a,d,#}, Lianliang Chen^{b,c,#}, Haoran Wang^{a,d}, Ziyang Shan^{a,d}, Zhengyang Zhou^{c,d}, Wenwei Li^{e,f}, Yang Wang^{a,c,*}

^aSchool of Software Engineering, University of Science and Technology of China, Hefei 230026, China.

^bAlibaba Inc., Hangzhou 310052, China.

^cSchool of Computer Science and Technology, University of Science and Technology of China, Hefei 230026, China.

^d188 RenAi Road, Suzhou Institute for Advanced Research, University of Science and Technology of China, Suzhou, Jiangsu 215123, China.

^eCAS Key Laboratory of Urban Pollutant Conversion, Department of Applied Chemistry, University of Science and Technology of China, Hefei 230026, China.

^fUSTC-CityU Joint Advanced Research Center, Suzhou, 215123, China.

* Corresponding author at 188 RenAi Road, Suzhou Industry Park, Suzhou, Jiangsu, 215123, China.

Wenjie Du and Lianliang Chen contributed equally to this manuscript.
E-mail address: angyan@ustc.edu.cn (Y. Wang).

1 **ABSTRACT**

2 Air pollution is a major obstacle to future sustainability, and traffic pollution has
3 become a large drag on the sustainable developments of future metropolises. Here,
4 combined with the large volume of real-time monitoring data, we propose a deep
5 learning model, iDeepAir, to predict surface-level PM_{2.5} concentration in Shanghai
6 megacity and linked with emission inventory creatively to decipher urban traffic
7 impacts on air quality. Our model exhibits high-fidelity in reproducing pollutant
8 concentrations and reduces the MAE by 20% compared with other models and
9 identifies the ranking of major factors. Local meteorological conditions have become a
10 nonnegligible factor. Layer-wise relevance propagation (LRP) is used here to enhance
11 the interpretability of the model and we visualized and analyzed the reasons for the
12 different correlation between traffic density and PM_{2.5} concentration in various regions
13 of Shanghai. Meanwhile, As the strict and effective industrial emission reduction
14 measurements implementing in China, the contribution of urban traffic to PM_{2.5}
15 formation is gradually increasing from 21.62% in 2010 to 35.67% in 2017 in Shanghai,
16 and the impact of traffic emissions would be ever-prominent in 2030 according to our
17 prediction. We also infer that the promotion of vehicular electrification would achieve
18 further alleviation of PM_{2.5} about 11.72% and reduce 11.72% by 2030 gradually. These
19 insights are of great significance to provide the decision-making basis for accurate and
20 high-efficient traffic management and urban pollution control, and eventually benefit
21 people's lives and high-quality sustainable developments of cities.

23 *Keywords:* PM2.5 concentration forecast; Traffic emissions; Deep learning;

24 Attention mechanism; New energy vehicles.

25

26

27 **1. Introduction**

28 Air pollution is a large obstacle to the world's future sustainable developments,
29 and millions of people die from air pollution-related diseases every year around the
30 world (Zheng *et al.*, 2017). This is seriously severe in some developing countries like
31 China (Lelieveld *et al.*, 2015), which has the highest country-level values globally for
32 the population-weighted annual average concentration of PM_{2.5} (Tichenor and Sridhar,
33 2019; Zhang *et al.*, 2012) and has been a major public health concern in recent years (Li
34 *et al.*, 2019a). Shanghai, one of the most developed and populous cities in China, has
35 suffered severe increasing haze episodes mostly attributed to the severe particle
36 pollution especially fine particles (particles $\leq 2.5\mu\text{m}$ in aerodynamic diameter; PM_{2.5})
37 (Li *et al.*, 2019a) since 1990s with the rapid urbanization and industrialization (Wang
38 *et al.*, 2015a). Under these circumstances, air pollution-related diseases have emerged
39 gradually, such as respiratory diseases in the elderly and preterm birth and low birth
40 weight for birth when maternal exposure to PM_{2.5} in Shanghai (Liu *et al.*, 2017).

41 Going further, the total number of vehicles in China has exceeded 200 million in
42 2019 and increases by more than 20 million annually in the urban. Vehicular traffic is a
43 principal source of air pollutants such as nitrogen oxides (NO_x), carbon monoxide (CO)
44 and carbonaceous particles (Zhang and Batterman, 2010). Traffic emission has become
45 one of the important factors affecting air quality due to the extensive motor vehicles in
46 China (Yan *et al.*, 2020). Meanwhile, some secondary pollutants discharged like O₃ ,
47 SO₂ and a major portion of PM_{2.5} are generally diverse in different regions and time
48 (Kroll *et al.*, 2020). When they involve different changes or conditions, they could

49 promote or alleviate the formation of PM_{2.5} in varying degrees such as high relative
50 humidity promoting the formation of PM_{2.5} (Benas *et al.*, 2013), higher temperature
51 enhancing the photochemical reaction in the atmosphere (Dumka *et al.*, 2015), wind
52 contributing greatly to diffuse particulate matter (Xiao *et al.*, 2011), which makes it
53 difficult to trace and analyze the causes of local air pollution and the major drivers (Le
54 *et al.*, 2020) in a specific area. Generally speaking, atmospheric chemical reactions
55 serve as essential nonlinear links between traffic emissions and atmospheric
56 composition (Yang *et al.*, 2021a; Zhu *et al.*, 2021). Meanwhile, local meteorological
57 factors, for instance, air temperature, wind-field (Zhou *et al.*, 2021), humidity, and so
58 on also strongly regulate photochemical formation of ozone and PM (Le, Wang, Liu,
59 Yang, Yung, Li and Seinfeld, 2020; Wu *et al.*, 2020; Yang, Wen, Wang, Zhang, Pinto,
60 Pennington, Wang, Wu, Sander, Jiang, Hao, Yung and Seinfeld, 2021a). Here, we
61 disentangle the complex factors involving emissions inventory, transport emission, and
62 meteorological conditions to evaluate the effect of different factors on air quality in
63 urban area by deep-learning.

64 To disentangle the complex factors, we focus on the issue of pollution tracing by
65 deep learning. Relatively speaking, traditional source **apportionment (SA) methods**
66 which mainly based on receptor-oriented model and source-oriented model (Huang *et*
67 *al.*, 2014; Zhang *et al.*, 2017), **are flawed for PM_{2.5} source identification and traffic**
68 **emission impact evaluation for the following reasons: a) most parameters in these**
69 **models, which are determined from the laboratory (Julie *et al.*, 2016), cannot accurately**
70 **reflect the real scene, and it is quite time-consuming to get these parameters; b) many**

71 important influential factors such as meteorological conditions, pollutant discharge,
72 secondary chemical substances formed during pollutants diffusion are not considered,
73 hence results in poor accuracy of the simulating results (Kumar *et al.*, 2018; Li *et al.*,
74 2017a; Souri *et al.*, 2016); c) the validity of quantifying impacts of different
75 anthropogenic emissions remains uncertain (Daskalakis *et al.*, 2016; Gao *et al.*, 2018;
76 Kumar, Peuch, Crawford and Brasseur, 2018). Compared with traditional chemical
77 transport modeling, the data-driven based data analysis method has more flexibility in
78 leveraging real-world data and could better fit nonlinear relationship (Yang *et al.*,
79 2021a; Zhu *et al.*, 2021) which has been considered as a new perspective to conduct
80 environment-related research in recent years (Alfaseeh *et al.*, 2020; Wang *et al.*, 2020)
81 since this technology is able to simulate complex pollution formation mechanisms by
82 focusing on data itself.

83 Some researchers think that deep learning is suitable for analyzing air
84 pollution(Hino *et al.*, 2018; Xing *et al.*, 2020), such as PM_{2.5} concentration prediction
85 via interpretable convolutional neural networks (Park *et al.*, 2020; Zhou, Zhang, Du and
86 Liu, 2021), assessing traffic impacts by random forest (Yang, Wen, Wang, Zhang, Pinto,
87 Pennington, Wang, Wu, Sander, Jiang, Hao, Yung and Seinfeld, 2021a), air quality
88 prediction in an image-based deep learning model (Zhang *et al.*, 2020). Actually, deep
89 learning technologies has demonstrated its strong ability and applied in multiple fields
90 including intelligent driving (Zhang *et al.*, 2018), intelligent medical (Li *et al.*, 2019b;
91 Lindsey *et al.*, 2018) , life science studies (Anonymous, 2019; Ham *et al.*, 2019; Yuan
92 and Bar-Joseph, 2019).

93 In order to enhance the interpretability of the model, Layer-wise relevance
94 propagation is used here. LRP (Bach *et al.*, 2015a), a method for explaining the
95 predictions of a broad class of machine learning models, has been widely applied and
96 well verified in many scenarios, such as machine translation, emotion analysis and text
97 classification text classification (Arras *et al.*, 2017a; Arras *et al.*, b; Ding *et al.*, 2017).
98 According to the contribution of neurons in the former layer to the latter layer, all
99 relevant values in the latter layer are allocated to the former layer and pushed back to
100 the input layer. In the process of pushing back, this follows the conservation principle
101 (Lapuschkin *et al.*, 2019).

102 In this paper, we propose a novel deep learning network, iDeepAir, to decipher the
103 impact of urban traffic on air quality by combining the multi source real-time data such
104 as traffic information, in situ surface-level pollutant concentrations and meteorology.
105 We assess the sensitivity of PM_{2.5} in Shanghai to traffic emission changes at different
106 stages by comparing predicted concentrations under different traffic emission scenarios.
107 Then, we utilize iDeepAir model to account for the nonlinear interactions among
108 different input parameters to fit the complex chemical reaction and temporal
109 accumulation procedure of PM_{2.5} formation. Furthermore, with the embedded LRP
110 algorithm (Bach, Binder, Montavon, Klauschen, Mueller and Samek, 2015a;
111 Lapuschkin, Waeldchen, Binder, Montavon, Samek and Mueller, 2019), the
112 contribution of each pollutant on the formation of PM_{2.5} can be quantified clearly and
113 separately which enhance the interpretability of the model. Moreover, to quantify the
114 contribution of anthropogenic emissions to PM_{2.5} development for each year from 2010

115 to 2017 we couple the emission inventories with the iDeepAir. And finally, considering
116 the development of new energy transportation policy and traffic emissions in the future,
117 we assess the possible benefits of future traffic evolution on PM_{2.5} reductions and derive
118 some potential impacts of new energy transportation policy in 2030.

119

120

121 **2. Material and methods**

122

123 2.1. Study area and datasets

124

125 Thanks to the development of environmental monitoring technology, we can
126 obtain a large number of historical monitoring data for academic research. The
127 iDeepAir model based on observation values connects multiple feature time series data
128 to predict PM_{2.5} concentration. The study focuses on Shanghai region, which is one of
129 the most developed area in China including 16 districts with different terrain and
130 population density. The location information of monitoring points and road network are
131 present in Fig.1.

132 The dataset used in this research consists of four parts: transportation-related
133 data, air quality data, meteorological data and pollutant emission load related data.
134 The detailed composition of the dataset and related statistical results are
135 presented in Table 1. (1) Transportation-related data. This dataset includes two
136 parts: Total numbers of both petrol and new energy vehicles and Traffic State

137 Indexes (TSIs). Total numbers of petrol and new energy vehicles, which are from
138 Shanghai Statistical Yearbook (<http://tjj.sh.gov.cn>) and Shanghai Traffic
139 Comprehensive Annual Report. TSIs, which can be obtained from Shanghai
140 Traffic Information Platform (<http://www.jtcx.sh.cn>), includes 68 traffic state
141 indexes reflecting the real-time traffic status in different regions of the city.
142 Regarding one specific region, this index is calculated with real-time road traffic
143 status that is collected from intraregional road segments every 2 minutes (Text
144 S1). (2) Air quality data. This data, which contains the hourly average monitored
145 air quality data of Shanghai, is collected from the Real-time Air Quality
146 Reporting System (<http://219.233.250.38:8087/AQI/siteAQI.aspx>). The detailed
147 elements of monitored data include Time, PM_{2.5}, PM₁₀, O₃, SO₂, NO₂, CO, and
148 all contaminant concentrations are recorded in micrograms per cubic meter
149 ($\mu\text{g}/\text{m}^3$). (3) Meteorological data. The meteorological data of Shanghai is
150 collected from the platform of Weather Underground, by taking the Shanghai
151 Hongqiao international Airport Monitoring Station as the reference point
152 (<https://www.wunderground.com/weather/ZSSS>). The detailed categories of
153 each meteorological record are shown in Table 1 and the sampling interval of
154 meteorological data is 30 minutes. (4) Pollutant emission load related data. The
155 annual total pollutant emission loads from the sectors of industry, resident, and
156 transportation can be found from Shanghai Municipal Statistics Bureau
157 (<http://tjj.sh.gov.cn>, <http://www.stats.gov.cn>). The annual generated electricity in
158 Shanghai, which can be used to infer the emissions of the power sector.

159 All data are one-hour interval, with a total of 5969 records. The datasets are
160 divided randomly into a training set (80%), and a test set (20%).

161

162 2.2. iDeepAir architecture

163

164 The iDeepAir adopts an encoder-decoder architecture, which consists of
165 three kinds of modules: Traffic Fusion Module (TFM), Feature Interaction
166 Module (FIM) and Time Interaction Module (TIM) (Fig. 2). (a) Traffic Fusion
167 Module. We employ an independent TFM to exploit the spatial dependence
168 between the road traffic status and air pollution with its multiple embedded
169 convolutional layers, and the results are combined with geographic information
170 to present the spatial distribution of the dependencies within traffic status and air
171 pollution. (b) Feature Interaction Module. In this module, we simulate the
172 complex chemical reactions between different contaminants by employing the
173 Multi-Head Attention structure(Vaswani *et al.*, 2017) to achieve the interactions
174 between different features. Considering that not all of these features can
175 contribute to the prediction of air pollution, we then introduce traditional
176 attention mechanism into this module to highlight key features. By combining
177 the self-attention and attention mechanism, this module can not only enable the
178 interactions between different features, but also can address sequential
179 forecasting problems with long-term dependency. Besides, this can achieve

180 higher accuracy forecasting. (c) Time Interaction Module. We use Temporal
181 Convolutional Network (TCN) to capture the long-term and deep interactions
182 between pollutant ingredients in the temporal dimension and simulate the
183 pollutant accumulation processes over time in chemical reactions with the inputs
184 of fine-grained meteorological records and learned feature interactions, and
185 finally generate the sequence of PM_{2.5} concentration in next 24 hours (Text S3).
186 TCN contains three sub-structures: causal convolution, dilation convolution and
187 residual connection (Text S3).

188

189 2.3. iDeepAir training algorithm

190 We implement and train the iDeepAir network with the deep learning
191 toolkits Keras (version 2.2.4) and Tensorflow (version 1.10.0) in Python (version
192 3.6.6). The training process is performed on Tesla V100-PCIE GPU, running
193 under the CentOS Linux 7 server. During the training phase, the batch size is 128
194 and the learning rate is 0.001. Adam optimizer is adopted and the objective loss
195 function is formulated as follows:

$$196 \quad \text{Loss} = \|\hat{y} - y\|_2^2$$

197 where \hat{y} and y are the predicted vector and the ground truth vector
198 respectively.

199

200 2.4. Evaluation methods

201

202 We use the mean absolute error (MAE), and Root Mean Squared Error
203 (RMSE) as the measurement to evaluate the prediction performance of our
204 proposed iDeepAir. Given a test set $Y = \{y_1, y_2, \dots, y_n\}$, the MAE and RMSE is
205 as follows:

$$206 \quad MAE = \frac{1}{n} \sum_{i=1}^n |\hat{y}_i - y_i|$$
$$207 \quad RMSE = \sqrt{\frac{1}{n} \sum_{i=1}^n |\hat{y}_i - y_i|^2}$$

208 where $\hat{Y} = \{\hat{y}_1, \hat{y}_2, \dots, \hat{y}_n\}$ is the set of the predicted value.

209

210 2.5. Layer-wise relevance propagation

211

212 Regarding a deep learning neural network, the input vector can be denoted
213 as $V = \{v_1, v_2, \dots, v_n\}$, and the prediction result of the network is $f(V)$, LRP
214 produces a decomposition $R = \{r_1, r_2, \dots, r_n\}$ of that prediction on the input
215 variables satisfying:

$$216 \quad \sum_{i=1}^n r_i = f(x)$$

217 The LRP method is based on a backward propagation mechanism applying
218 uniformly to all neurons in the network. By employing the LRP method on our

219 iDeepAir network, we then obtain the relevance between all 5 pollutants and the
220 output, and denote these as $\{r_0, r_1, r_2, r_3, r_4\}$.

221

222 2.6. Calculations of emission inventory

223

224 Based on the annual total pollutant emission loads of industrial, residential
225 and transportation sectors, the emission loads of SO₂, NO₂, CO, PM₁₀, and PM_{2.5}
226 from these three sectors can be directly calculated with considering the
227 proportional relationship among sulphur content, nitrogen content, and carbon
228 content within fuel. Further, based on the annual generated electricity in
229 Shanghai, the emission load of power sector can be calculated by:

230
$$\varepsilon_{energy}^{year} = e_g^{year} * \lambda$$

231 where $\varepsilon_{energy}^{year}$ corresponds to the emission loads from power sector in a
232 specific year, e_g^{year} indicates the generated electricity in that year, and λ is the
233 emission factor of generated electricity.

234

235 2.7. Quantifying contribution of emission sources

236

237 Assuming c_i is the contribution of the i -th emission source (Here $i \in$
238 $\{0,1,2,3\}$), and we have

239
$$c_i = \frac{\sum_{k=0}^4 p_i^k r_k}{\sum_{i=0}^3 \sum_{k=0}^4 p_i^k r_k}$$

240 Here p_i^k is the value of k _th pollutant component discharged by the i _th
241 emission source from the emission inventories.

242

243 2.8. Prediction of future contribution of traffic emissions

244

245 Based on the total numbers of petrol vehicles in Shanghai from 2010 to 2019,
246 we first learn the growth regularity of the total number of urban petrol vehicles
247 with regression analysis, and the regression equation can be written as (Fig.S1):

248
$$v_{year}^p = 26.569 \times (year - 2009) + 111.81$$

249 where variable $year$ indicates the year for prediction, and v_{year}^p
250 corresponds to the predicted number of petrol vehicles in the year for prediction.

251 Also, we can predict the number of Electrified vehicles in Shanghai based on
252 regression analysis on the historical numbers of new energy vehicles during
253 2013-2019, the regression equation is (Fig.S2):

254
$$v_{year}^n = 0.4634 \times (year - 2012)^2 + 1.162 \times (year - 2012) - 2.0102$$

255 where variable $year$ also means the year for prediction, and v_{year}^n is the
256 predicted number of new energy vehicles in the year for prediction. By
257 combining the contributed average $PM_{2.5}$ concentration of transportation
258 emissions from 2010 to 2017 with the actual number of petrol vehicles in

259 Shanghai during the same time, we then learned the regression equation which
260 represents the correlations among these two kinds of dataset (Fig.S3):

$$261 \quad p_{transportation}^{year} = 0.3054 \times (v_{year}^p)^{0.6885}$$

262 where $p_{transportation}^{year}$ is the predicted average PM_{2.5} concentration that
263 traffic emission contributes in the year for prediction. And if we replace the
264 variable v_{year}^p with v_{year}^n , this equation can be easily used to calculate the
265 PM_{2.5} reductions caused by the promotion of new energy vehicles in a
266 corresponding year.

267

268 **3. Results and discussion**

269

270 3.1. Evaluations of iDeepAir on PM_{2.5} predictions

271

272 In this subsection, the performance of iDeepAir on simulating the dynamic
273 spatiotemporal generation and evolution processes of urban air pollution can be
274 evaluated by measuring its accuracy on future PM_{2.5} concentration prediction (Fig. 3a).
275 Besides, we compared our model with several alternative neural networks for sequence
276 forecasting including ARIMA (Autoregressive integrated moving average (Box and
277 Pierce, 1970)), GBDT (Gradient Boosting Regression Tree(Friedman, 2001)) and
278 emerging deep learning based methods including LSTM (Long-short-term-memory
279 network(Hochreiter and Schmidhuber, 1997)), GRU (Gated Recurrent Unit(Cho *et al.*,

280 2014)), Seq2seq (Sequence to sequence(Sutskever *et al.*, 2014)), DA-RNN (Dual-stage
281 Attention-based Recurrent Neural network(Yao *et al.*, 2017)), ADAIN (Neural
282 Attention Model for Urban Air Quality Inference (Cheng *et al.*, 2018)), Geo-MAN
283 (Multi-level-attention-based RNN Model for Time Series Prediction(Liang *et al.*,
284 2018)). These methods use the same dataset, but the input data could be adjusted for
285 different models (Text S2).

286 The results of models for PM_{2.5} concentration prediction in different time periods
287 (+6h, +12h, +24h, +48h) are presented in Table 2. The best results are marked in bold.
288 Obviously, the results demonstrate that our iDeepAir outperforms other alternative
289 solutions in each prediction task, particularly in short-term predictions, iDeepAir has a
290 great prediction effect with the least MAR and RMSE. Totally, these models tend to
291 have greater inaccuracies in long-term prediction (+24h, +48h) but iDeepAir has a
292 better prediction accuracy compared with other baselines. **Specifically, compared to the**
293 **baseline of ARIMA, iDeepAir can reduce the MAE from 30.252 $\mu\text{g}/\text{m}^3$ to 16.961 $\mu\text{g}/\text{m}^3$**
294 **(Table 2 and Fig. 3b)**. Besides, we further discover that those hierarchical structured
295 networks such as seq2seq, DA-RNN, ADAIN, and Geo-MAN, can significantly surpass
296 those non-hierarchical structured networks, and this explains the superiority of our
297 hierarchical iDeepAir which is carefully designed based on the prior knowledge of the
298 dynamic formation process of PM_{2.5} (firstly the vehicle exhaust is discharged into the
299 atmosphere to affect the pollutant concentration data of the atmosphere, and then the
300 generation of PM_{2.5} is enhanced or offset under different meteorological conditions).
301 To verify the effectiveness of each module and the robustness of the model, we conduct

302 a series of ablation studies by removing and replacing each module of the integrated
303 iDeepAir framework. It can be observed that existed modules can effectively improve
304 the performance of the integrated model independently. These experiments verify the
305 predictive ability and robustness of the algorithm under different time lengths, and
306 reflects the practicality and stability (Fig. 3c).

307 In terms of verifying the accuracy of future PM_{2.5} concentration prediction,
308 iDeepAir has a distinct advantage with high fidelity. In addition, an important output
309 of iDeepAir is a ranking of the contributions of single parameter to the prediction in
310 LRP method (take the 24-hour prediction results as an example) (Bach *et al.*, 2015b)
311 (Fig. 3d). For PM_{2.5}, the five major governing factors are air quality, wind direction,
312 weather conditions, pressure and wind speed which are mainly some meteorological
313 factors. Secondary pollutants like O₃, and NO₂ and traffic emission are also important
314 precursors of PM_{2.5} (Wang *et al.*, 2015b) which are also important influence factors.
315 Some open source such as urban dust, soil dust, and cement dust could directly affect
316 the air quality, and then they remain in the air or are not completely removed, which
317 would still promote or inhibit the formation of PM_{2.5} in the future (L *et al.*, 2014).
318 Besides, the formation of PM_{2.5} is correlated to wind direction and wind speed due to
319 the dilution or aerial migration effect and slightly decreased as pressure increases
320 because of the change of air pressure will lead to the movement of air flow, which
321 would contribute to the diffusion of pollutants (Li *et al.*, 2017b; Liu *et al.*, 2020). As
322 the variation of meteorological conditions, secondary pollutants or precursor gases (e.g.
323 sulfate, nitrate, ammonium and carbonaceous matters) are essential to participate in the

324 generation of PM_{2.5} through photo-chemical reactions forming ozone and biogenic
325 VOC (volatile organic compound) to cause the severe PM_{2.5} pollution in Shanghai
326 megacity (Wang, Qiao, Lou, Zhou, Chen, Wang, Tao, Chen, Huang, Li and Huang,
327 2015b). Furthermore, weather condition is a key factor by changing solar irradiance
328 that is a limiting factor that influences ozone-related photochemistry (Parker *et al.*, 2020;
329 Pusede *et al.*, 2014; Yang *et al.*, 2021b). Such a ranking of influencing factors of PM_{2.5}
330 formation is comparatively consistent with current research (Su *et al.*, 2020; Yang, Wen,
331 Wang, Zhang, Pinto, Pennington, Wang, Wu, Sander, Jiang, Hao, Yung and Seinfeld,
332 2021a).

333

334 3.2. Spatial contribution from crucial domain on air quality

335

336 Combined with the spatial location of Shanghai, we analyzed the correlation
337 between traffic flow and PM_{2.5} in the mesh division of 16×16 . With the embedded
338 Layer-wise Relevance Propagation (LRP) algorithm, the spatial traffic emissions are
339 located and tracked clearly. The overall spatial patterns of urban traffic follow a core-
340 peripheral distribution, and Huangpu district, which lies in the core area of Shanghai,
341 is the most congested district in the city. In addition, there are two minor cores in
342 Baoshan District and Pudong New District respectively (Fig. 4a). Regarding Huangpu
343 district which is highly-developed, the more traffic emissions due to its developed

344 economy and the less diffusion caused by its internal skyscrapers will definitely lead to
345 more serious air pollution.

346 The spatial correlation between urban traffic and PM_{2.5} concentration is shown
347 with a citywide heat-map in Fig. 4b. As observed, there exist strong positive spatial
348 correlations within traffic patterns and PM_{2.5} concentration (Circled blue and marked
349 A). And most significant correlations are focused on the west side of Huangpu River
350 since this area has more focused traffic flows. Besides, in the central area of the city,
351 there exist two interesting sub-regions (Circled green and marked B) where the traffic
352 flow is relatively high while the correlations are inconspicuous. Through practical field
353 investigations, we discover most of these sub-regions are parklands and the heights of
354 most buildings in these two sub-regions are relatively low, and infer that this kind of
355 specific land properties could effectively accelerate the diffusion of air pollution, hence
356 reduce the impacts of traffic emissions on pollution. Furthermore, there exist some
357 particular sections (Circled black and marked C) with conflicting heavy traffic and
358 scarce correlations. Considering the industrial distribution of Shanghai, we believe the
359 correlations between urban traffic and PM_{2.5} concentration have been masked by the
360 dominant industrial emissions (Wang *et al.*, 2014a).

361

362 3.3. Calculate Emission inventory from 2010 to 2017

363

364 Based on the released emission loads of different pollutants from anthropogenic
365 sources and the generated electricity in Shanghai from 2010 to 2017, we calculate and
366 reconstruct the emission inventories for Shanghai for each year from 2010 to 2017 (Fig.
367 S4). During these years, the industrial emissions were always the source with the
368 highest emission load, and the transportation sector was the second-highest emission
369 source. Moreover, the emission loads of the industrial and power sectors decreased
370 significantly with the strictest industrial emission limitation measurements ever such as
371 simultaneous desulfurization and denitrification since 2013 as the consequence of clean
372 air actions (Tang *et al.*, 2019; Zhang *et al.*, 2019). However, even though strict license
373 plate limitation policy and vehicle emission standard had been employed during these
374 years, the emission load of transportation sector decreased laxly and limitedly since the
375 absolute total number of vehicles increased with great rapidity. Based on the calculated
376 emission inventories, we also discovered that the total emission loads of the key
377 pollutants of CO, NO₂, and SO₂ have been reduced by 59.81%, 72.03%, and 60.93%
378 respectively, and the air pollution limitation measurements that Shanghai had employed
379 were quite effective. Given the unsatisfactory transportation emission reductions, we
380 should increase our efforts in this regard (Fig. 5a).

381

382 3.4. Quantified contribution of anthropogenic emissions to PM_{2.5} formation

383

384 Based on the surveilled air quality data of Shanghai, we decompose the final
385 prediction results in terms of the input features with the embedded LRP algorithm of
386 iDeepAir, and cooperating this learned relevance with the calculated emission
387 inventories, the contribution of anthropogenic emissions to PM_{2.5} formation could be
388 directly and separately calculated (Fig. 5b). As demonstrated, the emission contribution
389 of the industrial, residential and power sectors to PM_{2.5} formation decreased steadily
390 and continuously, while the contribution of traffic emissions increased independently
391 and smoothly (Fig. 5a). We believe that the effectiveness of the strictest industrial and
392 power emission limitation measurements has been verified. Given the fact that industry
393 and power will be stick to these limitation measurements chronically, we should
394 definitely take the issue of reducing traffic emissions as the priority in subsequent
395 efforts on sustainably improving urban air quality.

396 To verify the correctness of our quantified contribution, we compared our results
397 with the official announced results. From an analysis report of PM_{2.5} source which was
398 publicly released by Shanghai Municipal Bureau of Ecology and Environment, the
399 traffic emissions accounted for 22.6%~33.6% of the total impacts of all local emissions
400 on PM_{2.5} formation in Shanghai, this report is generated with some previous mentioned
401 methods(Wang *et al.*, 2014b; Wang *et al.*, 2006; Yao *et al.*, 2002) which distinguish the
402 impacts of different emissions. In our calculation, transportation emissions accounted
403 for 22.69% and 24.35% of the total impacts of all local emissions on PM_{2.5} formation
404 (Fig. 5a) respectively in 2012 and 2013, and this is quite consistent with the official
405 released report.

406

407 3.5. Prediction of contribution of transportation emissions in future and Air quality
408 benefit for future new energy vehicle promotion

409

410 By learning the current growth rates of the total petrol and new energy vehicle
411 numbers in Shanghai from historical dataset, the current vehicle license plate limitation
412 and new energy promotion policies, we first estimate the possible total numbers of both
413 petrol and new energy vehicles in future (Fig. 6a). As predicted, the numbers of both
414 traditional petrol and new energy vehicles increase significantly during the next ten
415 years, and even though the absolute number of new energy vehicles may be up to 1.69
416 million, they may only account for a small part of 21.63% of total urban vehicles in
417 2030. Meanwhile, we use a power function to approximate the relationships between
418 with the actual numbers of petrol vehicles and the real contributed $PM_{2.5}$ concentration
419 of transportation emissions during 2010-2017, and use this approximated function to
420 predict the possible contributed $PM_{2.5}$ concentration of urban traffic in the following
421 ten years. Afterward, to be fair, we assume that no further limitation measurements will
422 be employed on reducing industrial and power emissions and the contributed
423 concentration of these two kinds of emissions are fixed for the next ten years, and the
424 contribution of urban petrol vehicles to $PM_{2.5}$ formation are calculated for the next ten
425 years (Fig. 6b). In 2030, the emissions from urban petrol vehicles may account for more
426 than 50% of the total impacts of all local emissions on $PM_{2.5}$ formation, and petrol
427 vehicle emissions will be the primary source of urban $PM_{2.5}$, and our initial conjecture

428 that the issue of reducing traffic emissions should be considered as the priority in
429 improving urban air quality is verified positively. Fortunately, we are delighted to
430 discover that the promotion of new energy vehicles may bring us an obvious reduction
431 on PM_{2.5} formation in 2030, considering the current fleet electrification promotion
432 policy and the possible contribution of petrol vehicle emissions to PM_{2.5}, which is a
433 very valuable solution.

434

435 3.6. Effectiveness evaluation of new energy vehicle promotion policies

436

437 Given the effectiveness of the promotion of new energy vehicles on PM_{2.5}
438 reductions and the giant prospective total number of petrol vehicles in 2030, it is a
439 realistic way to alleviate urban air pollution by improving the promotion of new energy
440 vehicles. We here evaluate the effectiveness of improving the promotion of new energy
441 vehicles on PM_{2.5} reductions (Fig. 6c). As shown, if 50% of all petrol vehicles are
442 replaced by new energy vehicles in 2030, the contribution of transportation emissions
443 to PM_{2.5} can be reduced by 11.72%, and the absolute value that traffic emissions
444 contribute to PM_{2.5} can be reduced from 25.33μg/m³ to 15.72μg/m³ (Fig. 6d). And the
445 reductions of transportation contribution on PM_{2.5} and the absolute traffic contributed
446 PM_{2.5} concentration can reach 25.24% and 8.36μg/m³ respectively in case that 80% of
447 all petrol vehicles are replaced by new energy vehicles. Based on this analysis, we

448 suggest that more forceful policies on enhancing the promotion of new energy vehicles
449 should be considered for greener and sustainable future developments of modern cities.

450

451 **4. Conclusions**

452

453 In this paper, we propose a novel method to quantify the influence of
454 anthropogenic emissions on $PM_{2.5}$ concentration with a novel and traceable deep
455 learning model. Our experiment results indicate that the proposed model could
456 achieve better fitting and prediction performances than the LSTM, GBRT,
457 Seq2Seq, DA-RNN model and other deep learning models. Furthermore, we
458 output the contributions of input parameter to the prediction in LRP method and
459 visualize and analyze the spatial correlation between traffic flow and $PM_{2.5}$.

460 In addition, we discover that transportation emissions will play the most
461 dominate role in future urban air pollution, and how to reduce traffic emissions
462 are an unavoidable issue on achieving sustainable developments in modern cities.
463 Meanwhile, to some extent, new energy vehicles can be considered as an
464 effective way to reduce traffic emissions. However, the current promotion
465 policies and efforts are far from enough. To further improve urban air quality, we
466 need some more effective and powerful measurements in response to the rapid
467 growth of urban traffic emissions.

468 Due to its powerful ability on simulating the complex chemical reaction and
469 temporal accumulation procedure of PM_{2.5} formation by integrating multi-source
470 data, the proposed deep learning network may be easily applied in other
471 metropolises to address the challenging pollution tasks. With the traceable deep
472 learning network, we can quantify the impacts of different anthropogenic
473 emissions on different urban air pollutants by computing jointly with local
474 emission inventories. To support more efficient and sustainable city planning, it
475 is very important to deeply and sufficiently understand the impacts of different
476 human activities on air pollution. The insights and observations obtained in this
477 paper are of great significance to provide the qualitative and quantitative
478 decision-making basis for citywide traffic management and urban pollution
479 control, and may eventually benefit people's lives and high-quality sustainable
480 developments of cities.

481 Last but not least, to fully address the challenge of urban air pollution,
482 multiple ingredients such as urban layout, industrial planning and population
483 distribution should be considered comprehensively in analyzing and tackling air
484 pollution, and the proposed deep learning network is capable of embedding these
485 heterogeneous features and learning the fine-grained influences of them on urban
486 air pollutions. For future research, if the organics of the emissions of different
487 human activities can be further considered (Guo *et al.*, 2020), the accuracy of
488 quantifying the impacts of different human activities can be subsequently
489 improved.

490

491 **Acknowledgements**

492

493 This paper is partially supported by the Anhui Science Foundation for
494 Distinguished Young Scholars (No.1908085J24), Natural Science Foundation of China
495 (No.62072427), Jiangsu Natural Science Foundation (No. BK20191193).

496

497 **Declaration of Competing Interest**

498 Wenjie Du and Lianliang Chen contributed equally to this manuscript. The authors
499 declared that there is no conflict of interest.

500

501 **Appendix A. Supplementary material**

502

503 Supplementary material has been submitted with this article.

504

505 **Data statement**

506

507 All datasets supporting this study are available from the corresponding authors
508 on reasonable request.

Table 1. Composition of the dataset and the related statistics.

Data Feature	Variable	Mean	Std	Min	Max	Time interval
Traffic data	TSI	28.39	9.13	5.83	50.64	2 min
Air quality	P _{2.5} ($\mu\text{g}/\text{m}^3$)	55.56	42.01	4	356.67	60 min
	PM ₁₀ ($\mu\text{g}/\text{m}^3$)	78.97	51.64	4.78	386.44	
	O ₃ ($\mu\text{g}/\text{m}^3$)	64.33	38.5	5.11	271	
	SO ₂ ($\mu\text{g}/\text{m}^3$)	20.14	13.91	6	125.56	
	NO ₂ ($\mu\text{g}/\text{m}^3$)	49.19	26.63	3.78	173.89	
	CO($\mu\text{g}/\text{m}^3$)	0.89	0.37	0.35	2.96	
Meteorological data	Weather conditions ^a	2.87	4.49	0	15	30 min
	Dew point temperature / $^{\circ}\text{C}$	9.04	9.48	-17	27	
	Humidity/%	69.56	18.19	14	100	
	Pressure/kPa	1019.23	8.36	994	1037	
	Temperature/ $^{\circ}\text{C}$	15.12	8.27	-3	37	
	Wind direction ^b	3.84	2.59	0	8	
	Wind speed/(m^*s^{-1})	13.95	6.53	3.6	43.2	
	Air quality ^c	2.02	1.02	1	6	
Time period	From 2014/8/11 to 2015/4/30					

510

a. The weather conditions has 16 features (sunny, overcast, sunny to cloudy, fog, sleet, thunder shower, light rain, heavy rain, moderate rain, rainstorm, heavy snow, light snow, moderate snow, rain, hail, cloudy), which are encoded into numerical variable [0,15].

511

512

513

b. The wind direction has 9 directions (no wind, north wind, west wind, east wind, south wind wind, northwest wind, northeast wind, etc.), which are encoded into numerical variable [0,8].

514

515

c. The air quality has six levels (I, II, III, IV, V, VI). The higher the index, the more serious the air pollution is, which

516

are encoded into numerical variable [1,6].

517

518

519 **Table 2. The result for hourly prediction values of PM2.5 of different models in**
520 **different time periods.**

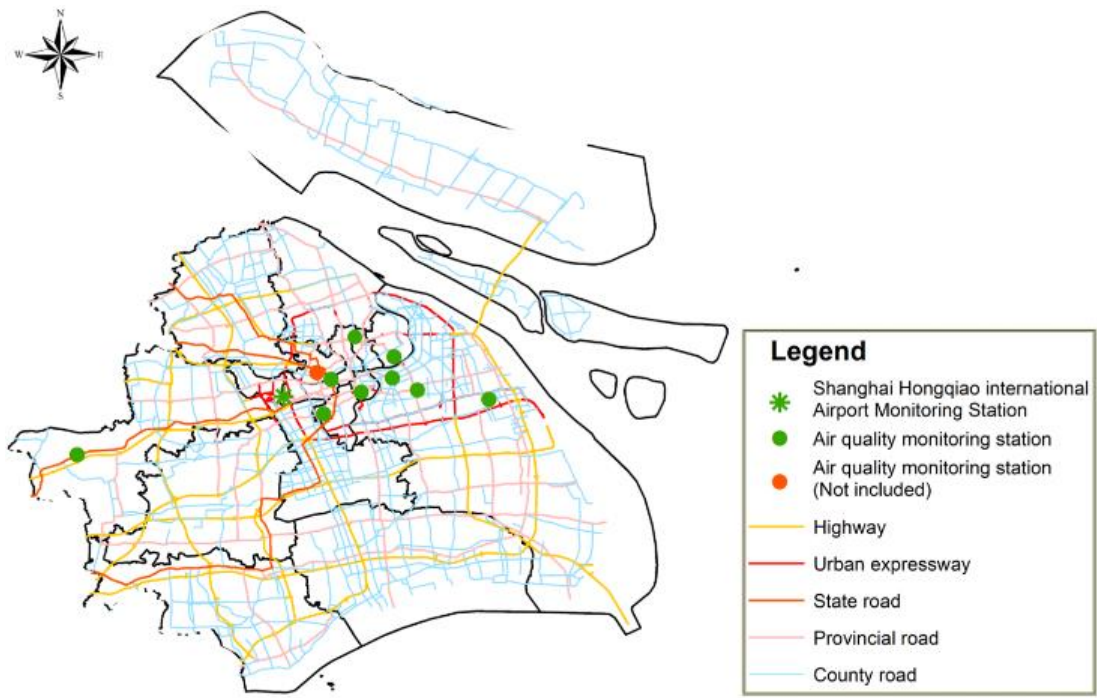
Method	+6h		+12h		+24h		+48h	
	RMSE	MAE	RMSE	MAE	RMSE	MAE	RMSE	MAE
ARIMA	38.649	28.562	38.634	27.805	41.150	30.252	37.753	27.593
GBDT	26.771	21.573	26.988	21.809	27.148	22.156	28.234	22.764
LSTM	25.830	20.176	27.164	21.721	31.690	23.779	33.495	25.466
GRU	24.321	20.017	26.248	20.963	30.546	22.979	32.879	22.856
Seq2Seq	19.685	14.946	24.966	19.653	28.708	22.816	29.419	23.012
DA-RNN	17.303	14.131	22.769	17.958	27.138	21.223	32.572	24.857
ADAIN	16.254	13.176	24.567	19.468	27.479	21.441	34.073	25.994
Geo- MAN	21.744	17.795	21.632	18.046	27.792	22.617	32.506	24.713
iDeepAir	5.849	11.825	20.285	15.890	23.233	16.961	24.595	19.891

521

522

523

524

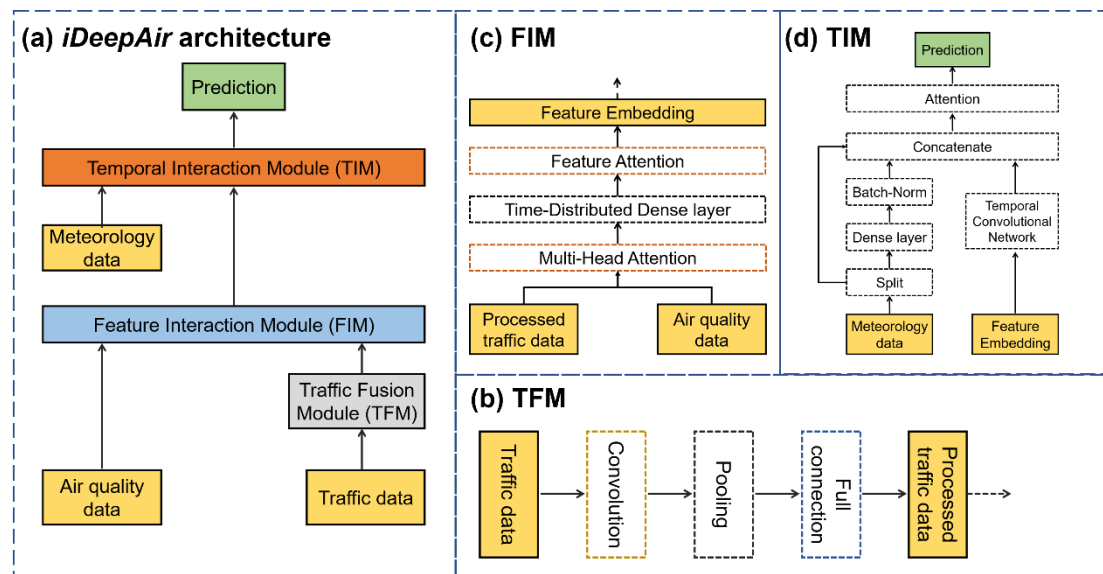


525

526

527

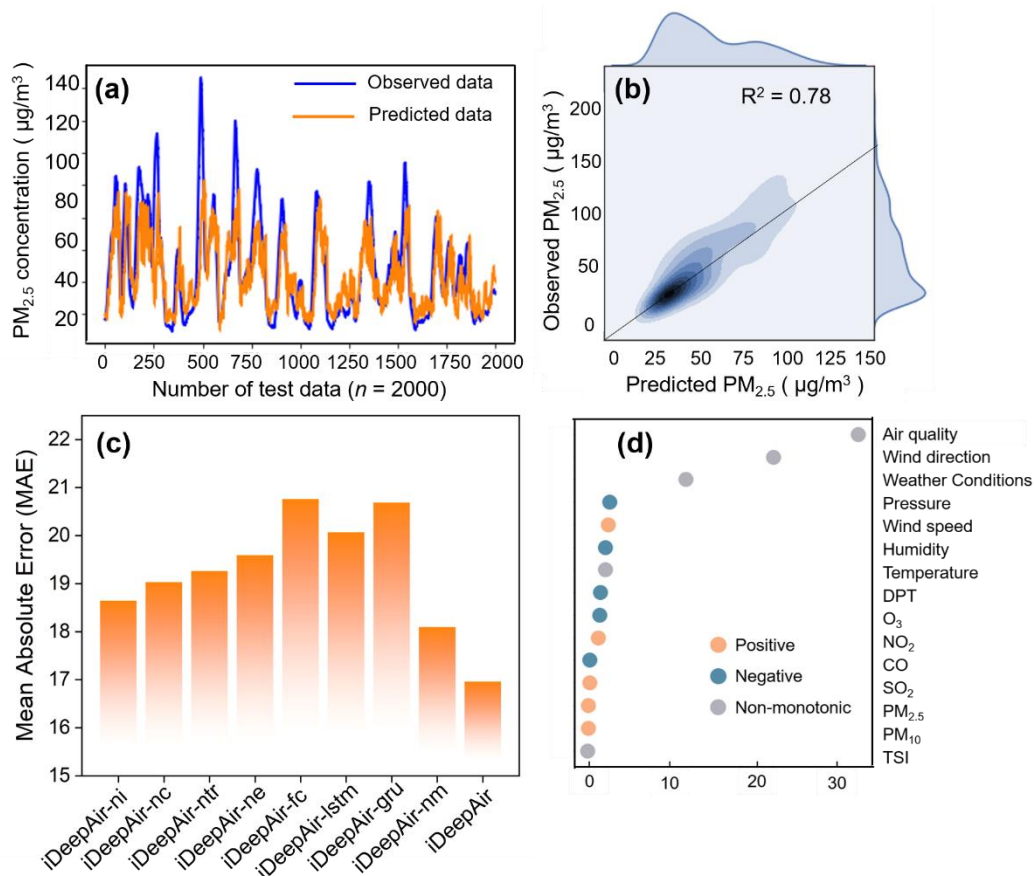
Figure 1. The spatial distribution of monitoring stations and road traffic network in Shanghai.



528

529 **Figure 2.** Overview of iDeepAir architecture and three important modules. (a) Overall
 530 hierarchical structure of iDeepAir, (b) Traffic Fusion Module (TFM), (c) Feature
 531 Interaction Module (FIM), and (d) Time Interaction Module (TIM).

532



533

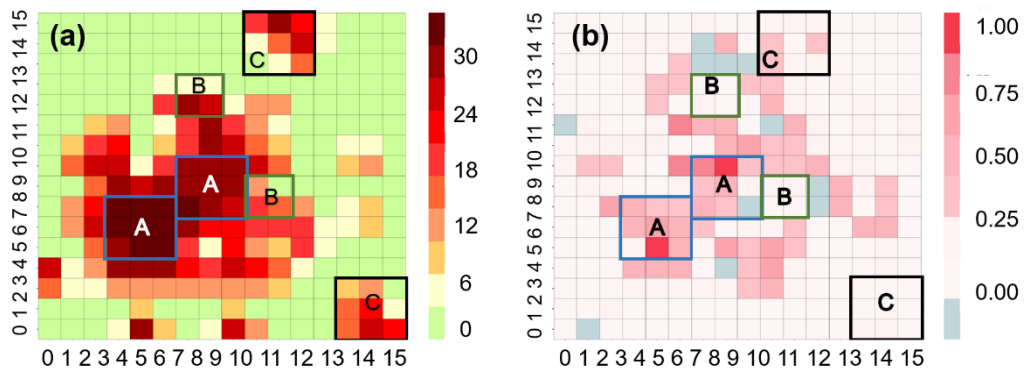
534 **Figure 3.** Model performance, ablative evaluations and variable contribution for PM_{2.5}

535 prediction. (a) and (b) The iDeepAir Model performance for PM_{2.5} prediction. (c)

536 Ablative evaluations of iDeepAir. (d) The Contribution assessment of variables (DPT:

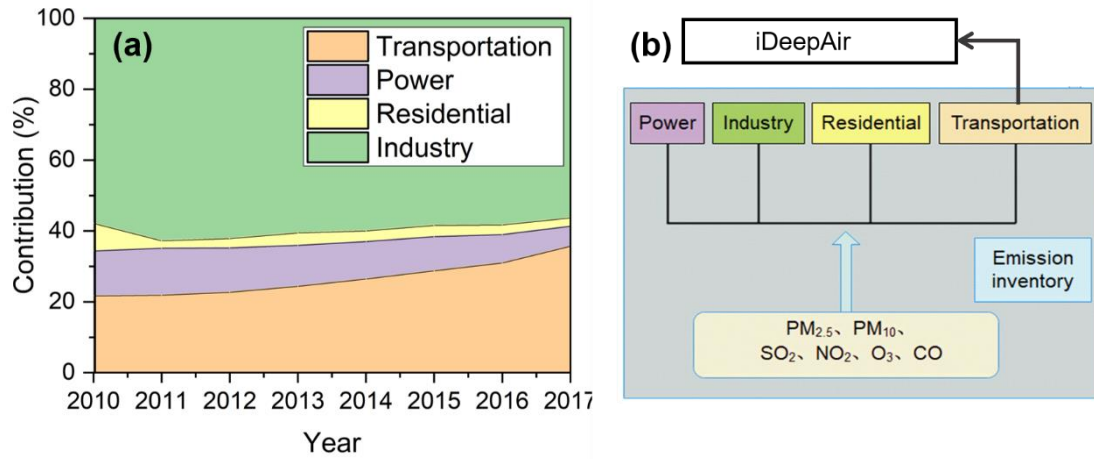
537 Dew point temperature).

538



539

540 **Figure 4.** Spatial distributions of average TSIs and correlations between traffic and
 541 PM_{2.5} in Shanghai. **(a)** Spatial distribution of average TSIs in Shanghai. **(b)** Spatial
 542 distribution of correlations between urban traffic and PM_{2.5} Concentration.



543

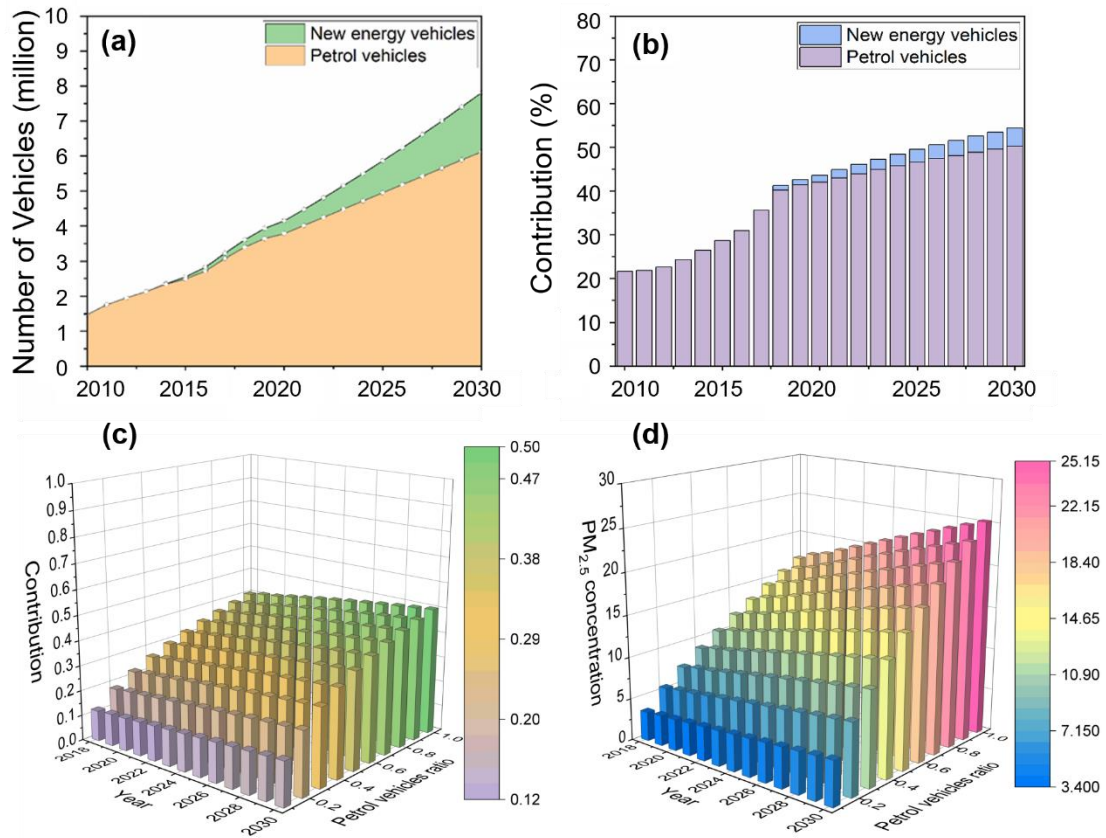
544 **Figure 5.** The contribution of anthropogenic emissions to PM_{2.5} formation in Shanghai.

545 **(a)** PM_{2.5} emission contribution rate of each industry (Transportation, Power,

546 Residential and Industry). **(b)** the overall framework of emission inventory and

547 iDeepAir model.

548



549

550 **Figure 6. Predictions of the total numbers of urban vehicles and evaluations of new**

551 **energy vehicle promotion from 2020 to 2030 in Shanghai. (a) Predictions of the total**

552 **numbers of both petrol and new energy vehicles from 2020 to 2030. (b) Predictions of**

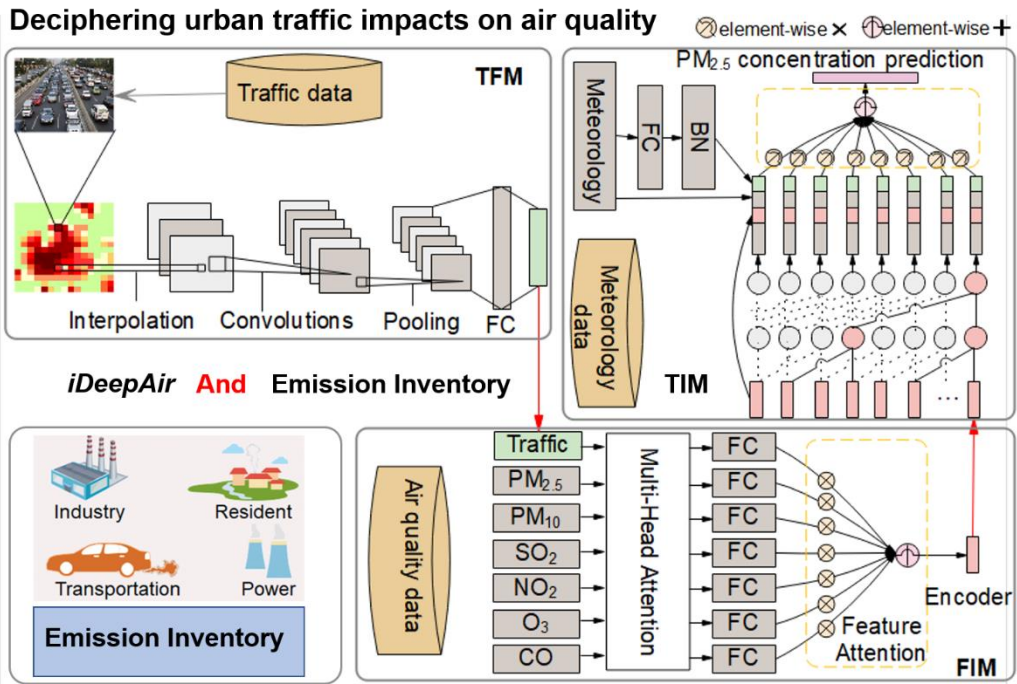
553 **the contribution of transportation emissions to PM_{2.5}. (c) Contribution of transportation**

554 **emissions to PM_{2.5} with different percentages of petrol vehicles replaced by new energy**

555 **vehicles. (d) PM_{2.5} concentration that transportation emissions contributed with**

556 **different percentages of petrol vehicles replaced by new energy vehicles.**

557



558

559

560

561

Table of Contents (TOC) graphic

562

563

参考文献

564 Alfaseeh, L, Tu, R, Farooq, B, Hatzopoulou, M, 2020. Greenhouse gas emission prediction on road
565 network using deep sequence learning. *Transport Res D-Tr E* 88(102593).

566 Anonymous, 2019. Deep learning monitors human activity based on sound alone. *Nature* 570(7759).

567 Arras, L, Horn, F, Montavon, G, Mueller, K, Samek, W, 2017a. "What is relevant in a text document?":
568 An interpretable machine learning approach. *Plos One* 12(e01811428).

569 Arras, L, Montavon, G, Muller, K R, Samek, W, 2017b. Explaining Recurrent Neural Network
570 Predictions in Sentiment Analysis [arXiv]. *arXiv*:9.

571 Bach, S, Binder, A, Montavon, G, Klauschen, F, Mueller, K, Samek, W, 2015a. On Pixel-Wise
572 Explanations for Non-Linear Classifier Decisions by Layer-Wise Relevance Propagation. *Plos One*
573 10(e01301407).

574 Bach, S, Binder, A, Montavon, G, Klauschen, F, Müller, K, Samek, W, 2015b. On Pixel-Wise
575 Explanations for Non-Linear Classifier Decisions by Layer-Wise Relevance Propagation. *Plos One*
576 10(7):e130140.

577 Benas, N, Beloconi, A, Chrysoulakis, N, 2013. Estimation of urban PM10 concentration, based on
578 MODIS and MERIS/AATSR synergistic observations. *Atmos Environ* 79:448-454.

579 Box, G E P, Pierce, D A, 1970. Distribution of Residual Autocorrelations in Autoregressive-Integrated
580 Moving Average Time Series Models. *Publications of the American Statistical Association*
581 65(332):1509-1526.

582 Cheng, W, Shen, Y, Zhu, Y, Huang, L, 2018. A Neural Attention Model for Urban Air Quality Inference:
583 Learning the Weights of Monitoring Stations, pp. 2151-2158.

584 Cho, K, van Merriënboer, B, Gulcehre, C, Bahdanau, D, Bougares, F, Schwenk, H, Bengio, Y, 2014.
585 Learning Phrase Representations using RNN Encoder-Decoder for Statistical Machine Translation.
586 *Computer Science*.

587 Daskalakis, N, Tsigaridis, K, Myriokefalitakis, S, Fanourgakis, G S, Kanakidou, M, 2016. Large gain in
588 air quality compared to an alternative anthropogenic emissions scenario. *Atmos Chem Phys*
589 16(15):9771-9784.

590 Ding, Y, Liu, Y, Luan, H, Sun, M, 2017. Visualizing and Understanding Neural Machine Translation, in
591 Barzilay R, Kan M Y (Eds.), pp. 1150-1159.

592 Dumka, U C, Kaskaoutis, D G, Srivastava, M K, Devara, P C S, 2015. Scattering and absorption
593 properties of near-surface aerosol over Gangetic-Himalayan region: the role of boundary-layer
594 dynamics and long-range transport. *Atmos Chem Phys* 15(3):1555-1572.

595 Friedman, J H, 2001. Greedy function approximation: A gradient boosting machine. *Ann Stat* 29(5):1189-
596 1232.

597 Gao, M, Han, Z, Liu, Z, Li, M, Xin, J, Tao, Z, Li, J, Kang, J, Huang, K, Dong, X, Zhuang, B, Li, S, Ge,
598 B, Wu, Q, Cheng, Y, Wang, Y, Lee, H, Kim, C, Fu, J S, Wang, T, Chin, M, Woo, J, Zhang, Q, Wang,
599 Z, Carmichael, G R, 2018. Air quality and climate change, Topic 3 of the Model Inter-Comparison
600 Study for Asia Phase III (MICS-Asia III) - Part 1: Overview and model evaluation. *Atmos Chem*
601 *Phys* 18(7):4859-4884.

602 Guo, S, Hu, M, Peng, J, Wu, Z, Zamora, M L, Shang, D, Du, Z, Zheng, J, Fang, X, Tang, R, Wu, Y,
603 Zeng, L, Shuai, S, Zhang, W, Wang, Y, Ji, Y, Li, Y, Zhang, A L, Wang, W, Zhang, F, Zhao, J, Gong,
604 X, Wang, C, Molina, M J, Zhang, R, 2020. Remarkable nucleation and growth of ultrafine particles

605 from vehicular exhaust. *P Natl Acad Sci Usa*.

606 Ham, Y, Kim, J, Luo, J, 2019. Deep learning for multi-year ENSO forecasts. *Nature* 573(7775):568.

607 Hino, M, Benami, E, Brooks, N, 2018. Machine learning for environmental monitoring. *NATURE*

608 *SUSTAINABILITY* 1(10):583-588.

609 Hochreiter, S, Schmidhuber, J, 1997. Long short-term memory. *Neural Comput* 9(8):1735-1780.

610 Huang, R, Zhang, Y, Bozzetti, C, Ho, K, Cao, J, Han, Y, Daellenbach, K R, Slowik, J G, Platt, S M,

611 Canonaco, F, Zotter, P, Wolf, R, Pieber, S M, Brunns, E A, Crippa, M, Ciarelli, G, Piazzalunga, A,

612 Schwikowski, M, Abbaszade, G, Schnelle-Kreis, J, Zimmermann, R, An, Z, Szidat, S, Baltensperger,

613 U, El Haddad, I, Prevot, A S H, 2014. High secondary aerosol contribution to particulate pollution

614 during haze events in China. *Nature* 514(7521):218-222.

615 Julie, Y Z, Chao, Z, Shi, Z, Li, V O K, Jiawei, H, Yu, Z, 2016. p-causality: identifying spatiotemporal

616 causal pathways for air pollutants with urban Big Data [arXiv]. *arXiv*:10.

617 Kroll, J H, Heald, C L, Cappa, C D, Farmer, D K, Fry, J L, Murphy, J G, Steiner, A L, 2020. The complex

618 chemical effects of COVID-19 shutdowns on air quality. *Nat Chem* 12(9):777-779.

619 Kumar, R, Peuch, V, Crawford, J H, Brasseur, G, 2018. Five steps to improve air-quality forecasts.

620 *Nature* 561(7721):27-29.

621 L, R, Z, Z, X, Z, W, Y, B, Y, Z, B, Y, J, 2014. Source Apportionment of PM10 and PM2.5 in Urban

622 Areas of Chongqing. *Research of Environmental Sciences* 27(12):1387-1394.

623 Lapuschkin, S, Waeldchen, S, Binder, A, Montavon, G, Samek, W, Mueller, K, 2019. Unmasking Clever

624 Hans predictors and assessing what machines really learn. *Nat Commun* 10(1096).

625 Le, T, Wang, Y, Liu, L, Yang, J, Yung, Y L, Li, G, Seinfeld, J H, 2020. Unexpected air pollution with

626 marked emission reductions during the COVID-19 outbreak in China. *Science (American*

627 *Association for the Advancement of Science)* 369(6504):702-706.

628 Lelieveld, J, Evans, J S, Fnais, M, Giannadaki, D, Pozzer, A, 2015. The contribution of outdoor air

629 pollution sources to premature mortality on a global scale. *Nature* 525(7569):367.

630 Li, M, Liu, H, Geng, G, Hong, C, Liu, F, Song, Y, Tong, D, Zheng, B, Cui, H, Man, H, Zhang, Q, He,

631 K, 2017a. Anthropogenic emission inventories in China: a review. *Natl Sci Rev* 4(6):834-866.

632 Li, T, Guo, Y, Liu, Y, Wang, J, Wang, Q, Sun, Z, He, M Z, Shi, X, 2019a. Estimating mortality burden

633 attributable to short-term PM2.5 exposure: A national observational study in China. *Environ Int*

634 125:245-251.

635 Li, X, Feng, Y J, Liang, H Y, 2017b. The Impact of Meteorological Factors on PM2.5 Variations in Hong

636 Kong. *IOP Conference Series: Earth and Environmental Science* 78:1-10.

637 Li, X, Wang, H, He, H, Du, J, Chen, J, Wu, J, 2019b. Intelligent diagnosis with Chinese electronic

638 medical records based on convolutional neural networks. *Bmc Bioinformatics* 20(62).

639 Liang, Y, Ke, S, Zhang, J, Yi, X, Zheng, Y, 2018. GeoMAN: Multi-level Attention Networks for Geo-

640 sensory Time Series Prediction.

641 Lindsey, R, Daluiski, A, Chopra, S, Lachapelle, A, Mozer, M, Sicular, S, Hanel, D, Gardner, M, Gupta,

642 A, Hotchkiss, R, Potter, H, 2018. Deep neural network improves fracture detection by clinicians. *P*

643 *Natl Acad Sci Usa* 115(45):11591-11596.

644 Liu, A, Qian, N, Yu, H, Chen, R, Kan, H, 2017. Estimation of disease burdens on preterm births and low

645 birth weights attributable to maternal fine particulate matter exposure in Shanghai, China. *Sci Total*

646 *Environ* 609:815-821.

647 Liu, T, Wang, X, Hu, J, Wang, Q, An, J, Gong, K, Sun, J, Li, L, Qin, M, Li, J, Tian, J, Huang, Y, Liao,

648 H, Zhou, M, Hu, Q, Yan, R, Wang, H, Huang, C, 2020. Driving Forces of Changes in Air Quality

649 during the COVID-19 Lockdown Period in the Yangtze River Delta Region, China. *Environ. Sci.*
650 *Technol. Lett.* 7(11):779-786.

651 Park, Y, Kwon, B, Heo, J, Hu, X, Liu, Y, Moon, T, 2020. Estimating PM_{2.5} concentration of the
652 conterminous United States via interpretable convolutional neural networks. *Environ Pollut*
653 256:113395.

654 Parker, H A, Hasheminassab, S, Crouse, J D, Roehl, C M, Wennberg, P O, 2020. Impacts of Traffic
655 Reductions Associated With COVID - 19 on Southern California Air Quality. *Geophys Res Lett*
656 47(23).

657 Pusede, S E, Gentner, D R, Wooldridge, P J, Browne, E C, Rollins, A W, Min, K E, Russell, A R, Thomas,
658 J, Zhang, L, Brune, W H, Henry, S B, DiGangi, J P, Keutsch, F N, Harrold, S A, Thornton, J A,
659 Beaver, M R, St. Clair, J M, Wennberg, P O, Sanders, J, Ren, X, VandenBoer, T C, Markovic, M Z,
660 Guha, A, Weber, R, Goldstein, A H, Cohen, R C, 2014. On the temperature dependence of organic
661 reactivity, nitrogen oxides, ozone production, and the impact of emission controls in San Joaquin
662 Valley, California. *Atmos Chem Phys* 14(7):3373-3395.

663 Souri, A H, Choi, Y, Jeon, W, Li, X, Pan, S, Diao, L, Westenbarger, D A, 2016. Constraining NO_x
664 emissions using satellite NO₂ measurements during 2013 DISCOVER-AQ Texas campaign. *Atmos*
665 *Environ* 131:371-381.

666 Su, T, Li, Z, Zheng, Y, Luan, Q, Guo, J, 2020. Abnormally Shallow Boundary Layer Associated With
667 Severe Air Pollution During the COVID - 19 Lockdown in China. *Geophys Res Lett* 47(20).

668 Sutskever, I, Vinyals, O, Le, Q V, 2014. Sequence to Sequence Learning with Neural Networks, in
669 Ghahramani Z, Welling M, Cortes C, Lawrence N D, Weinberger K Q (Eds.), *Advances in Neural*
670 *Information Processing Systems*.

671 Tang, L, Qu, J, Mi, Z, Bo, X, Chang, X, Anadon, L, Wang, S, Xue, X, Li, S, Wang, X, Zhao, X, 2019.
672 Substantial emission reductions from Chinese power plants after the introduction of ultra-low
673 emissions standards. *Nat Energy* 4:1-10.

674 Tichenor, M, Sridhar, D, 2019. Metric partnerships: global burden of disease estimates within the World
675 Bank, the World Health Organisation and the Institute for Health Metrics and Evaluation. *Wellcome*
676 *open research* 4:35.

677 Vaswani, A, Shazeer, N, Parmar, N, Uszkoreit, J, Jones, L, Gomez, A N, Kaiser, L, Polosukhin, I, 2017.
678 Attention Is All You Need, in Guyon I, Luxburg U V, Bengio S, Wallach H, Fergus R, Vishwanathan
679 S, Garnett R (Eds.), *Advances in Neural Information Processing Systems*.

680 Wang, A, Xu, J, Tu, R, Saleh, M, Hatzopoulou, M, 2020. Potential of machine learning for prediction of
681 traffic related air pollution. *Transport Res D-Tr E* 88(102599).

682 Wang, H L, Qiao, L P, Lou, S R, Zhou, M, Chen, J M, Wang, Q, Tao, S K, Chen, C H, Huang, H Y, Li,
683 L, Huang, C, 2015a. PM 2.5 pollution episode and its contributors from 2011 to 2013 in urban
684 Shanghai, China. *Atmos Environ* 123:298-305.

685 Wang, H L, Qiao, L P, Lou, S R, Zhou, M, Chen, J M, Wang, Q, Tao, S K, Chen, C H, Huang, H Y, Li,
686 L, Huang, C, 2015b. PM 2.5 pollution episode and its contributors from 2011 to 2013 in urban
687 Shanghai, China. *Atmos Environ* 123:298-305.

688 Wang, Y, Li, L, Chen, C, Huang, C, Huang, H, Feng, J, Wang, S, Wang, H, Zhang, G, Zhou, M, Cheng,
689 P, Wu, M, Sheng, G, Fu, J, Hu, Y, Russell, A G, Wumaer, A, 2014a. Source apportionment of fine
690 particulate matter during autumn haze episodes in Shanghai, China. *J. Geophys. Res. Atmos.*
691 119(4):1903-1914.

692 Wang, Y, Li, L, Chen, C, Huang, C, Huang, H, Feng, J, Wang, S, Wang, H, Zhang, G, Zhou, M, Cheng,

693 P, Wu, M, Sheng, G, Fu, J, Hu, Y, Russell, A G, Wumaer, A, 2014b. Source apportionment of fine
694 particulate matter during autumn haze episodes in Shanghai, China. *J Geophys Res-Atmos*
695 119(4):1903-1914.

696 Wang, Y, Zhuang, G, Zhang, X, Huang, K, Xua, C, Tang, A, Chen, J, An, Z, 2006. The ion chemistry,
697 seasonal cycle, and sources of PM_{2.5} and TSP aerosol in Shanghai. *Atmos Environ* 40(16):2935-
698 2952.

699 Wu, J, Bei, N, Hu, B, Liu, S, Wang, Y, Shen, Z, Li, X, Liu, L, Wang, R, Liu, Z, Cao, J, Tie, X, Molina,
700 L T, Li, G, 2020. Aerosol - photolysis interaction reduces particulate matter during wintertime
701 haze events. *Proc Natl Acad Sci USA* 117(18):9755-9761.

702 Xiao, Z, Zhang, Y, Hong, S, Bi, X, Jiao, L, Feng, Y, Wang, Y, 2011. Estimation of the Main Factors
703 Influencing Haze, Based on a Long-term Monitoring Campaign in Hangzhou, China. *Aerosol Air*
704 *Qual Res* 11(7):873-882.

705 Xing, J, Zheng, S, Ding, D, Kelly, J T, Wang, S, Li, S, Qin, T, Ma, M, Dong, Z, Jang, C, Zhu, Y, Zheng,
706 H, Ren, L, Liu, T, Hao, J, 2020. Deep Learning for Prediction of the Air Quality Response to
707 Emission Changes. *Environ Sci Technol* 54(14):8589-8600.

708 Yan, L, Luo, X, Zhu, R, Santi, P, Wang, H, Wang, D, Zhang, S, Ratti, C, 2020. Quantifying and analyzing
709 traffic emission reductions from ridesharing: A case study of Shanghai. *Transport Res D-Tr E*
710 89(102629).

711 Yang, J, Wen, Y, Wang, Y, Zhang, S, Pinto, J P, Pennington, E A, Wang, Z, Wu, Y, Sander, S P, Jiang,
712 J H, Hao, J, Yung, Y L, Seinfeld, J H, 2021a. From COVID-19 to future electrification: Assessing
713 traffic impacts on air quality by a machine-learning model. *Proc Natl Acad Sci USA*
714 118(26):e2102705118.

715 Yang, K, Kong, L, Tong, S, Shen, J, Chen, L, Jin, S, Wang, C, Sha, F, Wang, L, 2021b. Double High-
716 Level Ozone and PM_{2.5} Co-Pollution Episodes in Shanghai, China: Pollution Characteristics and
717 Significant Role of Daytime HONO. *Atmosphere-Basel* 12(5):557.

718 Yao, Q, Dongjin, S, Haifeng, C, Wei, C, Guofei, J, Cottrell, G, 2017. A Dual-Stage Attention-Based
719 Recurrent Neural Network for Time Series Prediction [arXiv]. *arXiv:7*.

720 Yao, X H, Chan, C K, Fang, M, Cadle, S, Chan, T, Mulawa, P, He, K B, Ye, B M, 2002. The water-
721 soluble ionic composition of PM_{2.5} in Shanghai and Beijing, China. *Atmos Environ* 36(PII S1352-
722 2310(02)00342-426):4223-4234.

723 Yuan, Y, Bar-Joseph, Z, 2019. Deep learning for inferring gene relationships from single-cell expression
724 data. *P Natl Acad Sci Usa* 116(52):27151-27158.

725 Zhang, K, Batterman, S, 2010. Near-road air pollutant concentrations of CO and PM_{2.5}: A comparison
726 of MOBILE6.2/CALINE4 and generalized additive models. *Atmos Environ* 44(14):1740-1748.

727 Zhang, Q, Fu, F, Tian, R, 2020. A deep learning and image-based model for air quality estimation. *Sci*
728 *Total Environ* 724.

729 Zhang, Q, He, K, Huo, H, 2012. Cleaning China's air. *Nature* 484(7393):161-162.

730 Zhang, Q, Zheng, Y, Tong, D, Shao, M, Wang, S, Zhang, Y, Xu, X, Wang, J, He, H, Liu, W, Ding, Y,
731 Lei, Y, Li, J, Wang, Z, Zhang, X, Wang, Y, Cheng, J, Liu, Y, Shi, Q, Yan, L, Geng, G, Hong, C, Li,
732 M, Liu, F, Zheng, B, Cao, J, Ding, A, Gao, J, Fu, Q, Huo, J, Liu, B, Liu, Z, Yang, F, He, K, Hao, J,
733 2019. Drivers of improved PM_{2.5} air quality in China from 2013 to 2017. *P Natl Acad Sci Usa*
734 116(49):24463-24469.

735 Zhang, X, Gao, H, Zhao, J, Zhou, M, 2018. 基于深度学习的自动驾驶技术综述. *清华大学学报. 自*
736 *然科学版* 58(1000-0054(2018)58:4<438:JYSDXX>2.0.TX;2-Z4):438-444.

-
- 737 Zhang, Y, Cai, J, Wang, S, He, K, Zheng, M, 2017. Review of receptor-based source apportionment
738 research of fine particulate matter and its challenges in China. *Sci Total Environ* 586:917-929.
- 739 Zheng, M, Yan, C, Wang, S, He, K, Zhang, Y, 2017. Understanding PM2.5 sources in China: challenges
740 and perspectives. *Natl Sci Rev* 4(6):801-803.
- 741 Zhou, H, Zhang, F, Du, Z, Liu, R, 2021. Forecasting PM2.5 using hybrid graph convolution-based model
742 considering dynamic wind-field to offer the benefit of spatial interpretability. *Environ Pollut*
743 273:116473.
- 744 Zhu, J, Deng, F, Zhao, J, Zheng, H, 2021. Attention-based parallel networks (APNet) for PM2.5
745 spatiotemporal prediction. *Sci Total Environ* 769:145082.
- 746